


RESEARCH

Open Access



# Neuronal MHC-I complex is destabilized by amyloid- $\beta$ and its implications in Alzheimer's disease

Min-Seok Kim<sup>1†</sup>, Kwangmin Cho<sup>1†</sup>, Mi-Hyang Cho<sup>1</sup>, Na-Young Kim<sup>1</sup>, Kyunggon Kim<sup>3</sup>, Dong-Hou Kim<sup>2\*</sup> and Seung-Yong Yoon<sup>1,2\*</sup> 

## Abstract

**Backgrounds** The expression of major histocompatibility complex I (MHC-I) in neurons has recently been shown to regulate neurite outgrowth and synaptic plasticity. However, its contribution to neurodegenerative diseases such as Alzheimer's disease (AD) remains largely unknown.

**Methods** In this study, we investigated the relationship between impaired MHC-I- $\beta$ 2M complex and AD in vitro and human AD samples. Interaction between protein was identified by liquid chromatography-tandem mass spectrometry and confirmed by immunoprecipitation. Single-chain trimer of MHC-I- $\beta$ 2M was generated to study the effect of stabilization of MHC-I- $\beta$ 2M complex on NCAM1 signaling.

**Results** MHC-I is destabilized in the brains of AD patients and neuronal cells treated with oligomeric  $\beta$ -amyloid (A $\beta$ ). Specifically, A $\beta$  oligomers disassemble the MHC-I- $\beta$ 2-microglobulin ( $\beta$ 2M) complex, leading to reduced interactions with neural cell adhesion molecule 1 (NCAM1), a novel interactor of neuronal MHC-I, and decreased signaling. Inhibition of MHC-I- $\beta$ 2M complex destabilization by non-dissociable MHC-I- $\beta$ 2M-peptide complex restored MHC-I-NCAM1 signaling in neuronal cells.

**Conclusions** The current study demonstrated that disruption of MHC-I-NCAM1 signaling by A $\beta$  induced disassembly of MHC-I- $\beta$ 2M complex is involved in the pathophysiology of AD. Moreover, our findings suggest modulation of MHC-I stability may be a potential therapeutic target for restoring synaptic function in AD.

**Keywords** Alzheimer's disease, MHC-I,  $\beta$ 2-microglobulin, NCAM1, High affinity peptide, Amyloid- $\beta$

## Introduction

Major histocompatibility complex I (MHC-I), a functional trimeric complex composed of MHC-I heavy chains,  $\beta$ <sub>2</sub>-microglobulin ( $\beta$ <sub>2</sub>M), and a short antigenic peptide, participates in the adaptive immune system by presenting intracellular antigenic peptides to cytotoxic T lymphocytes [1]. Although MHC-I is expressed in all the nucleated cells and was extensively studied in immune systems, less was known about MHC-I in the nervous system because brain was thought to be an immune-privileged organ. However, it began to be reported that MHC-I is also expressed in neurons of developing and

<sup>†</sup>Min-Seok Kim and Kwangmin Cho have contributed equally to this work.

\*Correspondence:

Dong-Hou Kim  
dhkim@amc.seoul.kr  
Seung-Yong Yoon  
ysy@amc.seoul.kr

<sup>1</sup> ADEL Institute of Science & Technology (AIST), ADEL, Inc., Seoul, Korea

<sup>2</sup> Department of Brain Science, Asan Medical Center, University of Ulsan College of Medicine, Seoul, Korea

<sup>3</sup> Department of Convergence Medicine, Convergence Medicine Research Center/Biomedical Research Center, Asan Medical Center, University of Ulsan College of Medicine, Seoul, Korea



adult brains [2], and is involved in the regulation of neurite outgrowth and synaptic plasticity in the central nervous system (CNS) [3]. MHC-I may also play a role in the regulation of initial synapse connections during CNS development [4–6], and in the regulation of synaptic density in the visual cortex and GABAergic synaptic density in cultured neurons [7]. Despite MHC-I's active role in CNS, little is known about its pathophysiological roles in various neurological and psychological diseases.

Although several meta-analyses of genetic risk factors for Alzheimer's disease (AD) have suggested that MHC-I alleles, specifically HLA-A2.1 [8] and HLA-B7 [9], are associated with AD pathology, the relationship between MHC-I with AD remains unclear because of contradictory reports in differential populations [10]. Amyloid- $\beta$  ( $A\beta$ ) peptide is a major pathological factor in synaptic dysfunction. Specifically, oligomeric  $A\beta$  dysregulates activity of several synaptic receptors.  $\alpha$ -amino-3-hydroxy-5-methyl-4-isoxazolepropionic acid (AMPA) and *N*-methyl-D-aspartate (NMDA) receptors, whose function and trafficking are regulated by synaptic MHC-I [11], are, in turn, negatively regulated by  $A\beta$  peptide in AD [12, 13]. Additionally, PirB which is a MHC-I receptor expressed in synapses of hippocampal neurons, and is involved in synaptic plasticity during CNS development [14–17], was identified as an amyloid- $\beta$  ( $A\beta$ ) receptor and has been implicated in AD pathology mediated by dysregulated synaptic plasticity with cofilin activation [18]. These findings suggest that MHC-I may have a putative role in AD pathophysiology.

We here addressed this point and revealed that  $A\beta$  destabilizes MHC-I complex resulting in decrease of NCAM-1 signaling but restoring MHC-I complex reverses its signaling in  $A\beta$ -treated neuronal cells.

## Materials and methods

### Human brain tissue

Medial temporal gyri from eight patients with AD and seven age- and sex-matched controls were provided by the Netherlands Brain Bank (Additional file 3: Table S1). AD pathological staging was based on the Braak staging system [19]. The hippocampus and cortex from the brains of normal controls and AD patients were analyzed by qRT-PCR, western blotting, synaptosome purification, and immunoprecipitation.

### DNA constructs

The DNA construct expressing the SCT of HLA-A2.1 (TAX-HLA-A2.1-h $\beta$ M) was the kind gift of Dr. Ted H. Hansen (Washington University School of Medicine, St. Louis, MO, USA). cDNAs encoding HLA-A2.1-WT and HLA-A2.1-SCT were amplified by polymerase chain reaction (PCR) and cloned into the mammalian expression

vector pcDNA3.1 (Invitrogen). Human NCAM1 cDNA was amplified by PCR from single-stranded cDNA synthesized from total RNA of normal human aged brain with a ReverTra Ace<sup>®</sup> qPCR RT kit (Toyobo Co., Ltd., Osaka, Japan), according to the manufacturer's protocol, and cloned into pcDNA3.1 vector. For N-terminus HA-tagging, a HA-Tag sequence was inserted behind the signal sequence region of NCAM1 by PCR.

### Cell culture and isolation of primary mouse cortical neurons

SH-SY5Y cells were maintained in Dulbecco's modified Eagle's medium (DMEM; Thermo Fisher Scientific Inc., Waltham, MA, USA) supplemented with 10% fetal bovine serum (FBS; Thermo Fisher Scientific Inc.), and incubated at 37 °C in an atmosphere containing 5% CO<sub>2</sub>. Cultures of primary cortical neurons were prepared from the brains of embryonic-day-16 pups, as described [20]. Briefly, the cerebral cortices were dissected in cold calcium- and magnesium-free Hank's balanced salt solution and incubated in 0.125% trypsin solution for 15 min at 37 °C. Trypsin was inactivated by the addition of DMEM containing 20% FBS, and cortical tissue was dissociated by repeated trituration using a Pasteur pipette. The cell suspensions were diluted in Neurobasal medium supplemented with B-27 components (Thermo Fisher Scientific Inc.), and seeded onto plates coated with poly-D-lysine (MilliporeSigma, Burlington, MA, USA) and laminin (1 mg/mL; Thermo Fisher Scientific Inc.). Neurons were maintained at 37 °C in a humidified 5% CO<sub>2</sub> environment.

### Immunocytochemistry

Primary cortical neurons ( $2 \times 10^5$  cells) were plated onto 18 mm coverslips (Paul Marienfeld GmbH & Co. KG, Lauda-Königshofen, Germany) coated with 0.05 mg/mL poly-D-lysine and 1  $\mu$ g/mL laminin (MilliporeSigma). The GFP construct was cotransfected with mock, wild-type (WT), or single chain trimer (SCT) HLA-A2.1 constructs into primary cortical neurons at 3 div using Lipofectamine 2000 (Thermo Fisher Scientific Inc.) according to the manufacturer's protocol. After 2 h, the cells were treated with  $A\beta$  oligomer for 48 h, fixed with 4% paraformaldehyde, and mounted onto slides for imaging. To assess the co-localization of MHC-I and NCAM1 or MHC-I and  $\beta_2$ M on primary neurons in the presence or absence of  $A\beta$  oligomer treatment, the cells were fixed and permeabilized with PBS containing 0.5% Triton X-100 for 10 min and incubated with blocking buffer (10% NGS, 5% bovine serum albumin [BSA], and 0.5% Tween 20 in PBS) for 1 h. The cells were subsequently incubated with primary anti-mouse MHC-I(B22-249.R1, Thermo Fisher Scientific Inc), anti-NCAM1(Proteintech) and anti- $\beta_2$ M(Abcam) antibodies overnight at 4 °C,

washed three times with PBS, and incubated with secondary Alexa fluor 488/594-conjugated anti-mouse or anti-rabbit antibody for 1 h at RT. The cells were again washed three times with PBS, stained with Hoechst 33,342 (Thermo Fisher Scientific Inc.) for 10 min, again washed with PBS, and mounted onto slides.

### Image analysis

Neurons and brain sections were examined with an LSM 780 confocal microscope (Carl Zeiss AG, Jena, Germany), and images were processed with ZEISS ZEN software (Carl Zeiss AG). For the quantitative analysis of neurite outgrowth, low-power magnified (10 $\times$ ) images of GFP-positive neurons were acquired from 20 different fields of view per sample and analyzed using MetaMorph software (Molecular Devices, LLC, San Jose, CA, USA). For the quantitative analysis of cells co-expressing MHC-I and  $\beta_2$ M or MHC-I and NCAM1, images of cells positive for both were acquired from 10 different field of view per sample from six mice.

### Coimmunoprecipitation and western blot analyses

For coimmunoprecipitation, purified synaptosomes (human/mouse), brain tissue (human/mouse), SH-SY5Y cells expressing NCAM1-HA, and cultured mouse cortical neurons were lysed with 1% digitonin (Millipore Sigma) containing 50 mM HEPES, 100 mM NaCl, 10 mM CaCl<sub>2</sub>, and 5 mM MgCl<sub>2</sub> (pH 7.6) supplemented with a protease inhibitor cocktail (Millipore Sigma) for 30 min at 4 °C. The lysates were precleared with protein G-sepharose (GE Healthcare, Little Chalfont, UK) for 1 h at 4 °C. Immunoprecipitation was performed by overnight incubation with anti-human MHC-I antibody (W6/32; Thermo Fisher Scientific Inc.), anti-mouse MHC-I antibody (2G5; Bio-Rad Laboratories, Inc., Hercules, CA, USA), or anti-HA antibody (11867423001, Roche Diagnostics Corporation, Indianapolis, IN, USA) at 4 °C. Immune complexes were purified using protein G-sepharose followed by three washes with 0.1% digitonin. Immunoprecipitated proteins were eluted by boiling in sodium dodecyl sulfate (SDS) sample buffer. Immunoprecipitated samples and 5% of the lysate preparations were electrophoresed on SDS-PAGE gels, which were stained with Coomassie blue or subjected to immunoblotting.

For western blot analyses, the protein lysates described above were homogenized in 1% Triton X-100 in PBS and incubated for 30 min at 4 °C. The preparations were centrifuged at 13,000 g for 15 min at 4 °C, and the protein concentrations in the supernatant were measured by Bradford assays. Protein samples were mixed with 5X SDS sample buffer [60 mM Tris-HCl (pH 6.8), 2% (w/v) SDS, 25% (v/v) glycerol, 14.4 mM (v/v)  $\beta$ -mercaptoethanol, and bromophenol blue], boiled for 5 min, and stored at

– 20 °C. The proteins were separated by 10% SDS–polyacrylamide gel electrophoresis (PAGE), transferred to polyvinylidene difluoride membranes (pore size, 0.2  $\mu$ m; Bio-Rad Laboratories, Inc.), and blocked with 5% (v/v) skim milk in 0.1% (v/v) Tween-20 in PBS (PBS-T) for 1 h at RT. The blots were incubated with primary antibodies overnight at 4 °C, washed three times in PBS-T buffer, and incubated with horseradish peroxidase-conjugated secondary antibodies for 1 h. The immunoblots were visualized using ECL reagents (Thermo Fisher Scientific Inc.). The primary antibodies used in the western blotting analyses were anti-human MHC-I (NBP2-66946, Novus Biologicals, LLC, Littleton, CO, USA); anti- $\beta_2$ M (Abcam plc, Cambridge, UK); anti-NCAM1 (14255-1-AP, Proteintech Group, Inc., Rosemont, IL, USA); anti- $\beta$ -actin (Millipore-Sigma); anti-protein disulfide isomerase (Thermo Fisher Scientific, Inc.); anti-mouse MHC-I (OX-18; Abcam plc); anti-PSD95, anti-synaptophysin, anti-glyceraldehyde 3-phosphate dehydrogenase (MilliporeSigma); and anti-ERp57, anti-tapasin, anti-TAP, anti-pCREB, anti-CREB, anti-c-fos, and anti-BDNF (Santa Cruz Biotechnology, Inc., Dallas, TX, USA). The band intensities were measured and analyzed with ImageJ software (<https://imagej.nih.gov/ij/>).

### Synaptosomes

Synaptosomes were purified as described [21]. Briefly, frozen human or mouse brain tissues were homogenized in isotonic sucrose buffer (0.32 M sucrose, 1 mM ethylenediaminetetraacetic acid, 5 mM Tris, pH 7.4) supplemented with protease inhibitor cocktail (MilliporeSigma) with 20 strokes of a Dounce homogenizer. The homogenates were centrifuged at 1,000 $\times$ g for 10 min at 4 °C. The supernatants were loaded onto Percoll (GE Healthcare) gradients (3%, 10%, 15%, and 23% in isotonic sucrose buffer) and ultracentrifuged at 31,000 $\times$ g for 5 min at 4 °C. All fractions were collected and analyzed by western blotting. For immunoprecipitation, the synaptosome pellets were lysed with 1% Triton X-100 in PBS supplemented with protease inhibitor cocktail for 30 min at 4 °C. The lysates were incubated with human anti-MHC-I antibodies [W6/32 (Thermo Fisher Scientific Inc.) or HC10 (OriGene Technologies, Inc., Rockville, MD, USA)] overnight at 4 °C, and the immunoprecipitates were purified on protein G-sepharose. The boiled eluents were analyzed by western blotting. To identify novel proteins that interacted with MHC-I, synaptosomes were prepared from the hippocampal region (1 g) of normal aged human brain.

### Bio-layer interferometry assay

Interactions between NCAM1 and MHC-I- $\beta_2$ M were analyzed using the BLItz<sup>®</sup> system (Pall ForteBio LLC,

Fremont, CA, USA), which measures bio-layer interferometry. To analyze the binding of NCAM1 and MHC-I- $\beta$ 2M, 100 nM of recombinant his-tagged NCAM1 protein (Abcam plc) was immobilized on a Ni-NTA biosensor (Pall ForteBio LLC), and the immobilized protein was incubated with the recombinant biotinylated stable form of MHC-I- $\beta$ 2M (HLA-A2.1 allele, MBL International Corporation, Woburn, MA, USA), diluted in PBS to concentrations of 0, 50, 100, 250, 500, and 1000 nM. Ligands (NCAM1 or MHC-I- $\beta$ 2M) were loaded onto biosensors for 120 s and washed. Binding of the ligand-analyte was monitored for 120 s, and the binding affinity was calculated by the BLItz<sup>®</sup> system.

### Flow cytometry

Cell-surface MHC-I expression was analyzed by flow cytometry. SH-SY5Y cells were incubated with oA $\beta$  for 24, 48, and 72 h. The cells were harvested, washed twice in cold PBS containing 1% BSA, and incubated with W6/32 or anti-HA antibody for 1 h at 4 °C. Labeled cells were washed twice in cold PBS containing 1% BSA and stained with FITC-conjugated goat anti-mouse IgG for 1 h at 4 °C. As a negative control, the cells were incubated with normal mouse IgG. In each sample, a total of 10,000 gated events were collected by FACSCanto II flow cytometer (BD Biosciences, San Jose, CA, USA) and analyzed with FACSDiva software (BD Biosciences).

### A $\beta$ peptide

A $\beta$  oligomers were prepared as described [20]. Briefly, lyophilized A $\beta$ <sub>1-42</sub> peptides (4014447, Bachem AG, Bubendorf, Switzerland) were dissolved in dimethyl sulfoxide (DMSO) to a final concentration of 500  $\mu$ M and diluted in DMEM to a final concentration of 1  $\mu$ M. Oligomeric A $\beta$  was prepared by incubating diluted monomeric A $\beta$  for 24 h at 4 °C. Untreated control are treated 0.2% DMSO.

### Quantitative real-time PCR

Total RNA was isolated from brain tissues of normal individuals and AD patients, from wild-type mouse brain tissues, and from A $\beta$ -treated SH-SY5Y cells using TRIzol (Thermo Fisher Scientific Inc.). Single-stranded cDNA was synthesized with a ReverTra Ace<sup>®</sup> qPCR RT kit according to the manufacturer's protocol. Quantitative reverse transcription-PCR (qRT-PCR) was performed using a LightCycler<sup>®</sup> 480 II (Roche Diagnostics Corporation) with iQ<sup>™</sup> SYBR<sup>®</sup> Green Supermix (Bio-Rad Laboratories, Inc.). The primers used for qRT-PCR included those for HLA-ABC (forward, 5'-GCCTAC GACGGCAAGGATTAC-3'; reverse, 5'-GGTGGCCTC ATGGTCAGAGA-3'), and glyceraldehyde 3-phosphate

dehydrogenase (forward, 5'-AATCCCATCA CCATCT TCC-3'; reverse, 5'-GGACTCCACG ACGTACTCA-3').

### Glycosylation analysis

Aged normal and AD brain tissues were homogenized in tissue extract buffer (1% Triton X-100, 50 mM Tris-HCl [pH 8.0], 150 mM NaCl, and 5 mM ethylenediaminetetraacetic acid supplemented with protease inhibitor cocktail). The lysates were incubated with W6/32 antibody for 2 h at 4 °C and then with protein G-sepharose. To analyze MHC-I glycosylation, immunoprecipitates were digested at 37 °C for 1 h with 3 mM endoglycosidase-H (Roche Diagnostics Corporation) or peptide-N-glycosidase F (New England BioLabs, Inc., Ipswich, MA, USA) according to the manufacturers' protocols. The beads were boiled in SDS sample buffer for 10 min and analyzed by immunoblotting.

### Cell-surface protein biotinylation

To investigate the changes in cell-surface MHC-I structure induced by A $\beta$ , SH-SY5Y cells were washed twice in cold PBS and incubated in cold PBS containing 10 mM sulfo-NHS-SS-biotin (Thermo Fisher Scientific Inc.) for 30 min at 4 °C. The cells were washed twice in cold PBS and quenched with 50 mM Tris-Cl (pH 8.0) before treatment with A $\beta$  for 1 h at 4 °C. The A $\beta$ -treated cells were lysed in 1% Triton X-100 in PBS supplemented with protease inhibitor cocktail (MilliporeSigma). The lysates were immunoprecipitated with anti-MHC-I antibodies (W6/32, which recognizes the MHC-I- $\beta$ 2M complex; and HC10, which recognizes free MHC-I) or streptavidin-agarose (Thermo Fisher Scientific Inc.). Culture media were also collected and immunoprecipitated with the anti- $\beta$ 2M antibody. The immunoprecipitates were analyzed by western blotting.

### In-gel digestion

The SDS-PAGE gels were sliced and chopped into small particles with a clean blade and destained with 200 mM ammonium bicarbonate (ABC) and 50% acetonitrile. The gel particles were dehydrated with 100% acetonitrile and washed with 50 mM ABC. The proteins in the gel were reduced with dithiothreitol at 70 °C for 20 min and alkylated with iodoacetamide at RT for 1 h. After washing with 50 mM ABC and 100% acetonitrile, the proteins in the gel were digested with sequencing grade trypsin (Promega Corporation, Madison, WI, USA) on resin at 37 °C overnight in digestion buffer (100 mM Tris pH 8.0 and 2 mM CaCl<sub>2</sub>), and the tryptic peptides were desalted using Sep-PAK C18 cartridges (Waters Corporation, Milford, MA, USA) and dried under vacuum in a SpeedVac.

### LC-MS/MS and sequence database analyses

Peptides were separated using the Dionex™ UltiMate™ 3000 RSLCnano system (Thermo Fisher Scientific Inc.). Tryptic peptides from the bead columns were reconstituted with 0.1% formic acid and separated on a 50 cm Easy-Spray™ column of inner diameter 75 μm packed with 2 μm C18 resin (Thermo Fisher Scientific Inc.) for over 120 min (300 nL/min) using a 0–45% acetonitrile gradient in 0.1% formic acid at 50 °C. The LC system was coupled to a Q Exactive mass spectrometer with a nano-ESI source. The mass spectra were acquired in a data-dependent mode with an automatic switch between a full scan with five data-dependent MS/MS scans. The target value for the full-scan MS spectra was 3,000,000, with a maximum injection time of 120 ms and a resolution of 70,000 at *m/z* 400. The ion target value for MS/MS was set to 1,000,000 with a maximum injection time of 120 ms and a resolution of 17,500 at *m/z* 400. Repeated peptides were dynamically excluded for 20 s. The resulting raw files were processed using MaxQuant (version 1.5.2.8), and the sequences were compared with those in the *Homo sapiens* database [organism ID: 9606, 71,567 entries, UniProt (<http://www.uniprot.org/>)]. The search parameters were set at default, including cysteine carbamidomethylation as a fixed modification; N-terminal acetylation, methionine oxidation, and phospho-serine, -threonine, and -tyrosine as variable modifications; and di-glycine modification at a lysine residue with two miscleavages. Peptide identification was based on a search with an initial mass deviation of the precursor ion of up to 10 ppm, and the allowed fragment mass deviation was set at 20 ppm. The resulting out files from MaxQuant were processed through Scaffold software (version 4.4.1.1; Proteome Software, Inc., Portland, OR, USA) for further statistical analyses and visualization.

### Statistical analysis

Quantitative data were analyzed statistically using GraphPad Prism 7 software (GraphPad Software, Inc., La Jolla, CA, USA). All data are presented as the mean ± the standard error of the mean (SEM), and analyzed by unpaired two-tailed Student's *t*-tests or by one-way or two-way ANOVA with Tukey's post-hoc comparisons tests. *P*-values < 0.05 were considered statistically significant. All experiments were repeated at least three times, and no data were excluded.

## Results

### Aβ-mediated downregulation of MHC-I stability in AD pathology

We first assessed whether Aβ affects MHC-I. SH-SY5Y cells were treated with Aβ oligomers for various time periods, and MHC-I levels were assessed by immunoblotting. Interestingly, Aβ treatment markedly reduced MHC-I levels (Fig. 1A) but MHC-I mRNA levels were unaffected (Fig. 1B), indicating that Aβ-mediated MHC-I downregulation occurred at the protein level. Since the protein stability, especially cell surface quality control, of MHC-I is mainly determined by its complex with antigen peptide and β2M [22], we checked the cell surface level of MHC-I-β2M complex, total MHC-I, with fluorescence-activated cell sorting (FACS) using W6/32 which detects only total human MHC-I, not free MHC-I unbound to β2M. Cell surface level of total MHC-I complexed with β2M was decreased by oligomeric Aβ treatment in a time-dependent manner (Fig. 1C), suggesting dissociation of β2M from MHC-I complex by Aβ oligomers. To investigate this point further, biotinylated cell-surface MHC-I-β2M complexes on SH-SY5Y cells treated with oligomeric Aβ for a short time were purified with specific monoclonal antibodies, either W6/32 or HC10, which recognizes the β2M-free human MHC-I [23, 24] to detect conformational changes in MHC-I-β2M by Aβ oligomers (Fig. 1D). The levels of biotinylated MHC-I-β2M complex

(See figure on next page.)

**Fig. 1** Oligomeric amyloid-β (Aβ) downregulated expression and structure of MHC-I-β<sub>2</sub>M complex. **A** Immunoblot analyses of MHC-I expression levels in Aβ oligomer (oAβ)-treated SH-SY5Y cells (left) The total MHC-I levels were normalized to those of GAPDH (**B**; n=4, one-way ANOVA with Tukey's post-hoc comparisons test) (right). **B** MHC-I mRNA levels in oAβ-treated SH-SY5Y cells (n=4, one-way ANOVA with Tukey's post-hoc comparisons test). **C** Surface MHC-I was labeled with the W6/32 antibody, analyzed by flow cytometry (n=4, one-way ANOVA with Tukey's post-hoc comparisons test). Representative histogram (left) and quantification of fluorescence intensity (right) of surface MHC-I-β<sub>2</sub>M complex. **D-H** Schematic representations of the structural changes in MHC-I-β<sub>2</sub>M complex detectable by different antibodies (W6/32 and HC10) and the release of surface β<sub>2</sub>M by oAβ-treated SH-SY5Y cells (**D**). Immunoprecipitation analysis of Aβ-induced structural changes in surface MHC-I-β<sub>2</sub>M complex (**E**; n=4). The levels of surface MHC-I-β<sub>2</sub>M complex (**F**) and surface-free MHC-I (**G**) were normalized to total surface MHC-I levels. The levels of released β<sub>2</sub>M were normalized to those of total β<sub>2</sub>M (**H**). The data were analyzed by unpaired two-tailed Student's *t*-test (**F-H**). (**I, J**) Immunoblot analyses of MHC-I levels in oAβ-treated SH-SY5Y cells in the presence or absence of the proteolytic inhibitors lactacystin (LC) and bafilomycin A1 (BFA1); n=4 (**I**), or the endocytosis inhibitors chlorpromazine (CPZ) and methyl-β-cyclodextrin (MβCD); n=4 (**J**). Total MHC-I levels were normalized to the levels of actin. The data were analyzed by one-way ANOVA with Tukey's post-hoc comparisons test (**I, J**). The data are presented as the mean ± SEM (N.S., not significant; \**P* < 0.05, \*\**P* < 0.001, \*\*\**P* < 0.005)

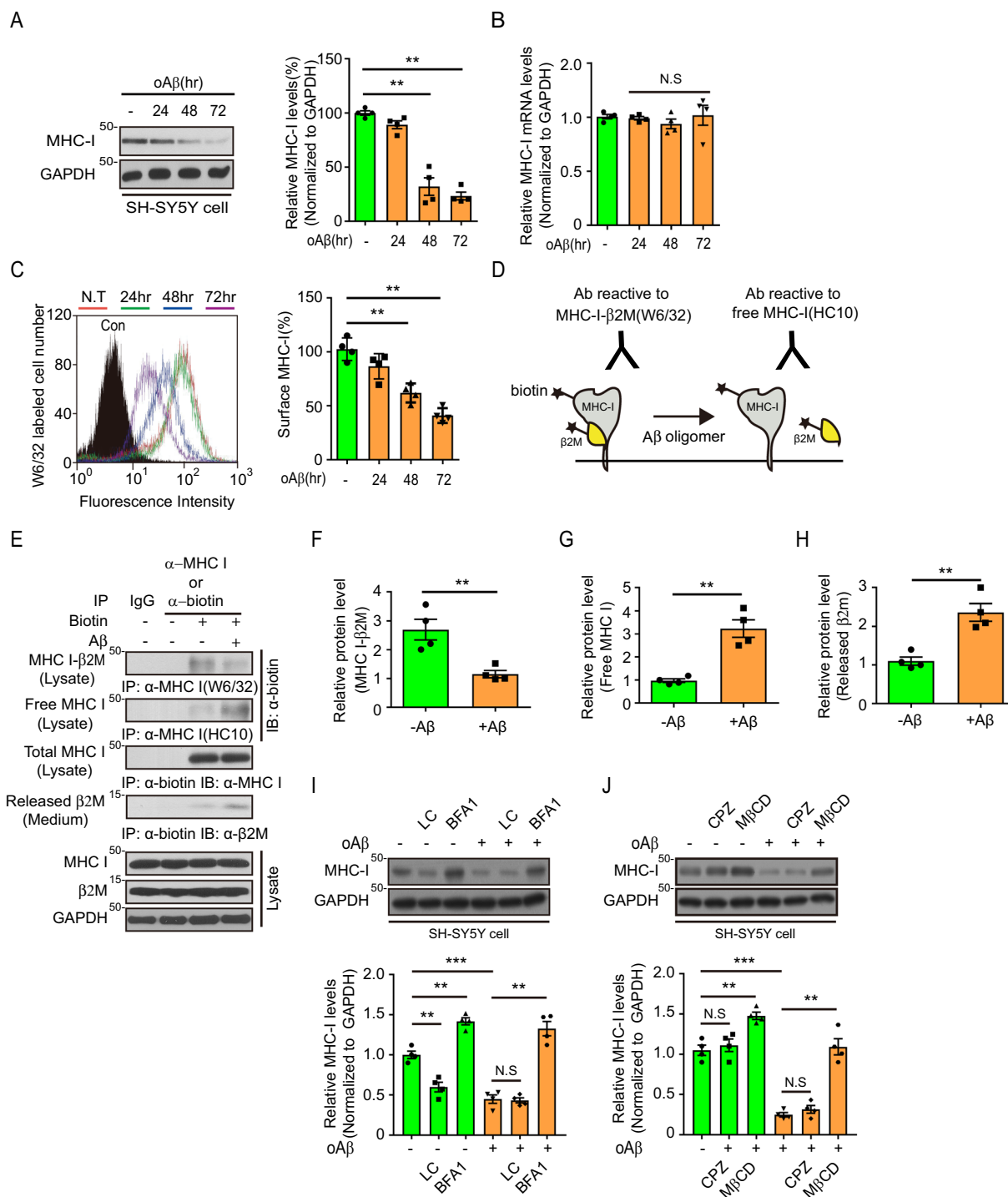


**Fig. 1** (See legend on previous page.)

reacting with W6/32 were reduced by 60% (Fig. 1E, F) in line with the FACS result (Fig. 1C), whereas the levels of biotinylated free heavy chain of MHC-I reacting with HC10 were increased threefold in Aβ-treated SH-SY5Y cells (Fig. 1E, G), suggesting that Aβ induced dissociation

of cell surface MHC-I-β2M complex. This Aβ-mediated destabilization of cell-surface MHC-I-β2M complex was confirmed by the increased extracellular release of β2M into the culture medium from MHC-I-β2M complex (Fig. 1E, H). Because the reduced stability of surface

MHC-I- $\beta$ 2M complex accelerates its endocytosis [25]. We investigated the intracellular pathways associated with A $\beta$ -mediated MHC-I downregulation. The change of total MHC-I levels was examined after A $\beta$  treated SH-SY5Y cells were treated with or without proteolysis inhibitors, either the proteasome inhibitor lactacystin or the lysosome inhibitor bafilomycin A1. MHC-I depletion was rescued by bafilomycin A1, but not by lactacystin, indicating that A $\beta$ -mediated MHC-I depletion requires lysosomal activity (Fig. 1I). In the absence of A $\beta$ , lactacystin directly reduced MHC-I levels by inhibiting proteasome activity, generating a peptide important for intracellular MHC-I folding. Because bafilomycin inhibited endocytic lysosomal degradation, the effects of endocytic pathway inhibitors, including the caveolin-dependent endocytosis inhibitor methyl- $\beta$ -cyclodextrin and the clathrin-dependent endocytosis inhibitor chlorpromazine, were also investigated. Methyl- $\beta$ -cyclodextrin increased MHC-I levels in the presence or absence of A $\beta$  treatment, whereas chlorpromazine had no effect on MHC-I levels under both conditions (Fig. 1J), suggesting that A $\beta$  enhances MHC-I endocytosis via a caveolin-dependent pathway followed by lysosomal degradation. Together, these observations suggested that the A $\beta$  oligomer has a novel deteriorating function, reducing the stability of MHC-I- $\beta$ 2M complex and stimulating lysosomal degradation of MHC-I.

#### Destabilization of MHC-I- $\beta$ 2M complex in AD brains

To investigate whether impaired MHC-I- $\beta$ 2M complex was involved in AD pathology, we investigated synaptic MHC-I levels in AD brains because functional neuronal MHC-I is mainly localized to the synapses [26, 27]. Among the hippocampal fractions in normal brains, almost 60% of total MHC-I was in the synaptic fractions (Fig. 2A, B), a finding confirmed by assessing the expression of several synaptic proteins, including synaptophysin, VGAT, and postsynaptic density (PSD)-95. NeuN, a neuronal nuclear protein, localized to the non-synaptic fractions, also confirming the purity of isolated synaptosomes. MHC-I and  $\beta$ 2M levels were reduced 50% in synaptic fractions of AD brains (Fig. 2A–C). The synaptic proteins including synaptophysin and PSD95 were also downregulated in AD synapses (Fig. 2A, D), indicating synaptic degeneration in AD brains [28, 29]. Higher PSD95 localization in non-synaptic fraction may reflect the shift in the distribution of PSD95 from post-synapse to other regions as disease progression [28]. Together, these results indicated that synaptic levels of MHC-I and  $\beta$ 2M are reduced in AD brains. Using two kinds of MHC-I conformation-specific antibodies, immunoprecipitation analysis demonstrated that most synaptic MHC-I in synaptosomes of control brains was present

in W6/32-sensitive MHC-I- $\beta$ 2M complex form (Fig. 2D, E). In AD synaptosomes, however, most synaptic MHC-I was present as HC-sensitive  $\beta$ 2M-free MHC-I heavy chains (Fig. 2D, F).

Since MHC-I- $\beta$ 2M complex formation was assisted by peptide-loading complex in the endoplasmic reticulum (ER) [30], we checked whether the destabilization of MHC-I- $\beta$ 2M complex is due to the impairment of complex formation in the ER. There were no changes in AD brains in the levels of proteins composing the ER folding machinery, including ERp57, protein disulfide isomerase (PDI), tapasin, and transporter associated with antigen processing (TAP) (Additional file 1: Fig. S1A, B). In addition, analysis of isolated MHC-I digested with endoglycosidase-H and peptide-N-glycosidase F showed that glycosylation maturation of MHC-I was not altered in AD brains (Additional file 1: Fig. S1C). These results suggest that intracellular folding and glycosylation maturation of MHC-I- $\beta$ 2M complex were not associated with destabilization of MHC-I- $\beta$ 2M complex in AD brains.

#### Identification of NCAM1 interactions with synaptic MHC-I- $\beta$ 2M complexes

Because the structural formation of MHC-I- $\beta$ 2M complex is critical for interaction with its functional counterpart, we hypothesized that a conformational change in MHC-I- $\beta$ 2M complex could alter its interactions with unknown synaptic proteins in AD. To identify proteins that interact with neuronal MHC-I, synaptic proteins binding to MHC-I- $\beta$ 2M complexes were co-purified with W6/32 antibody from the synaptosomes of normal human brain and analyzed with a proteomics approach. In addition to detecting several proteins in synaptosomes previously shown to interact with MHC-I- $\beta$ 2M complex, including GRP78, calnexin, and  $\beta$ -COP [31–33], liquid chromatography-tandem mass spectrometry (LC-MS/MS) identified a 150 kDa protein that interacted with the stable form of MHC-I (Fig. 3A, Additional file 2: Fig. S2A–C, Additional file 3: Table S2). This protein was subsequently identified as NCAM1, a transmembrane glycoprotein that regulates neurite outgrowth, synaptogenesis, and synaptic plasticity [34–37]. This NCAM1-MHC-I interaction was confirmed by immunoblotting of the same synapse fraction with antibody to NCAM1 (Fig. 3B) and by its coimmunoprecipitation from SH-SY5Y cells expressing HA-tagged NCAM1 (Fig. 3C, D). The NCAM1-MHC-I interaction was further confirmed by a bio-layer interferometry assay using recombinant NCAM1 and MHC-I- $\beta$ 2M complex, with binding affinity of  $K_D$  of 31.3 nM (Fig. 3E). Therefore, NCAM1 was identified as a novel interactor of MHC-I in human brain synaptosome.

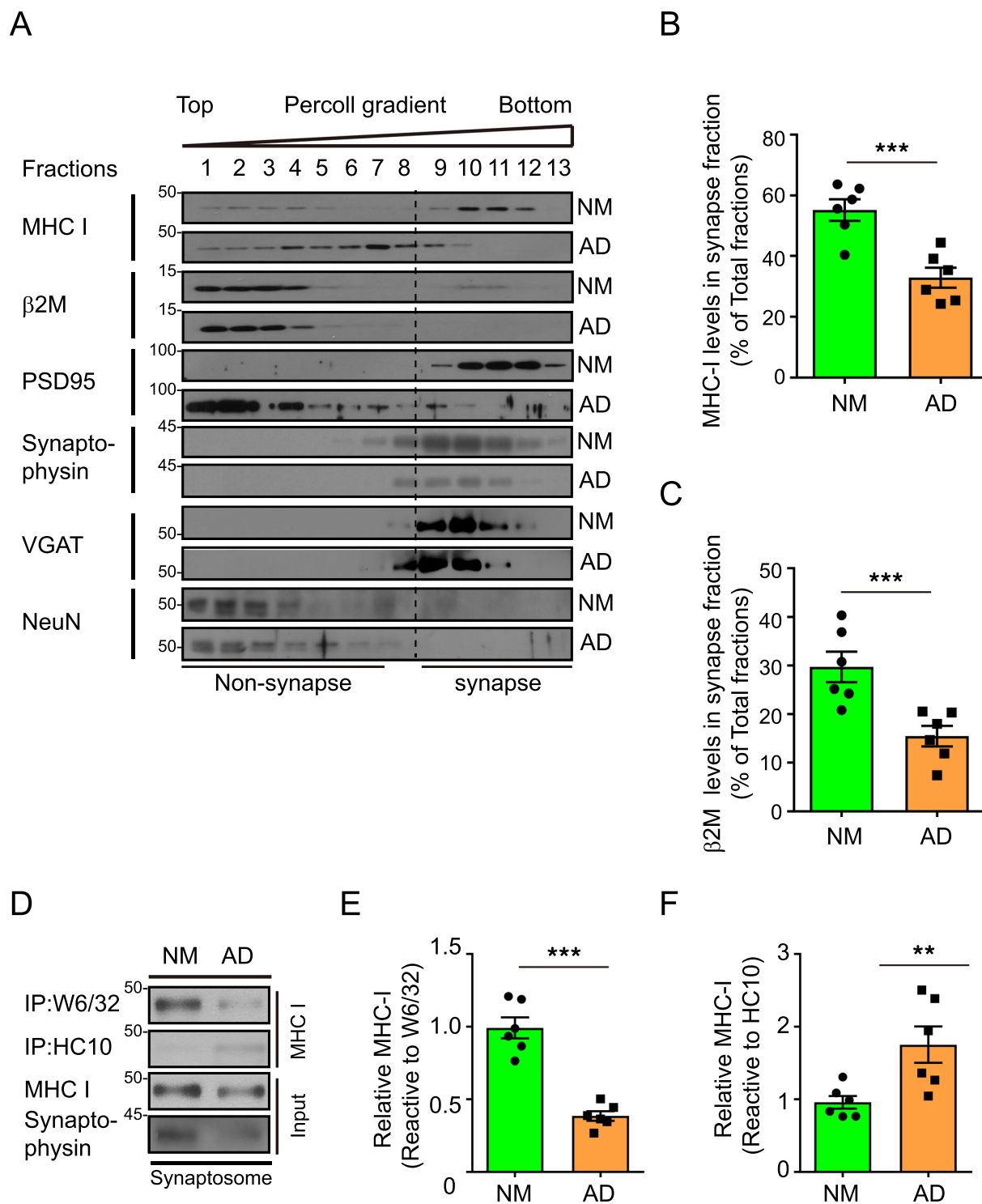


**Fig. 2** Pathologic changes of neuronal MHC-I-β<sub>2</sub>M complex in the brains of AD patients. **A–C** Immunoblot analyses of MHC-I, β<sub>2</sub>M, PSD95, synaptophysin, VGAT, and NeuN in subcellular fractions from aged normal and AD brains. The levels of MHC-I (**B**) and β<sub>2</sub>M (**C**) in synaptosomes were normalized to total protein levels in all fractions (n = 6). **D–F** Immunoprecipitation analyses with specific antibodies of MHC-I-β<sub>2</sub>M complex and β<sub>2</sub>M-free MHC-I in synaptosomes purified from aged normal and AD brains (**C**: n = 6). The levels of the purified β<sub>2</sub>M interacting (**E**) and β<sub>2</sub>M-free (**F**) forms of MHC-I in synaptosomes were normalized to total protein levels. Data are presented as the mean ± standard error of the mean (SEM) (N.S., not significant; \*P < 0.05, \*\*P < 0.001 by unpaired two-tailed Student’s t-test)



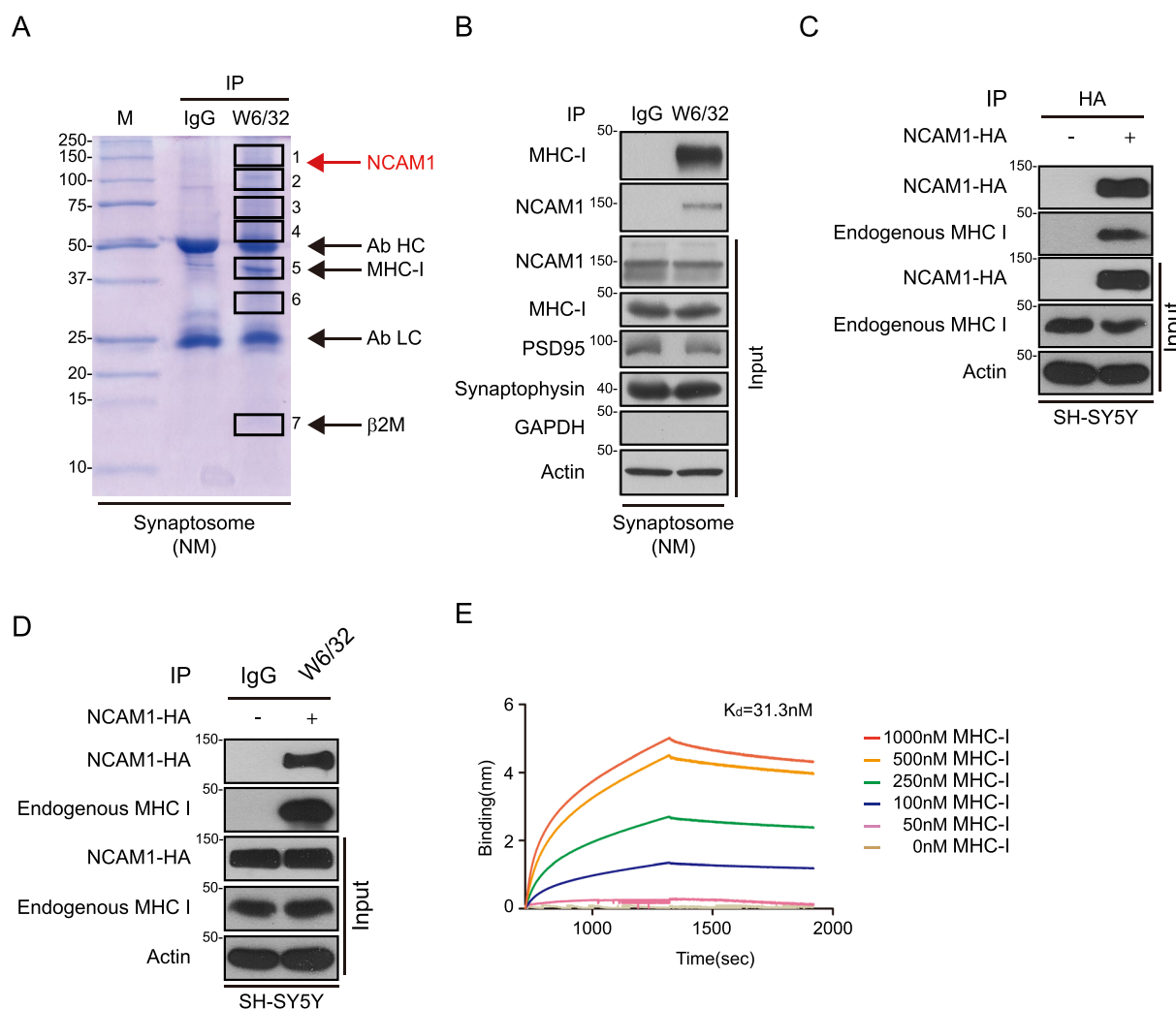


**Fig. 3** Identification of NCAM1 as a novel neuronal MHC-I interacting protein. **A** Proteins in synaptosomes from normal aged human brain that interacted with MHC-I, as shown by coimmunoprecipitation with W6/32 antibody and staining with Coomassie blue. Gel slices 1–7 were processed by in-gel digestion and LC–MS/MS analysis. **B** Confirmation of the MHC-I–NCAM1 interaction by immunoblotting with antibodies to MHC-I and NCAM1. Synaptosome purity was assessed by immunoblotting with antibodies to PSD95, synaptophysin, and GAPDH. **C, D** Coimmunoprecipitation analysis of the interaction between NCAM1 and MHC-I. Lysates of SH-SY5Y cells expressing NCAM1-hemagglutinin (HA) were immunoprecipitated with antibodies to HA (**C**) and W6/32 (**D**), followed by immunoblotting with the anti-HA and anti-MHC-I antibodies (**C, D**). The blots are representative of three independent experiments. **E** Bio-Layer Interferometry analysis of the affinity of interaction between MHC-I and NCAM1. NCAM1 protein (100 nM) was immobilized onto a biosensor, which was incubated with recombinant biotinylated MHC-I– $\beta_2$ M complex (HLA-A2.1 allele) at concentrations of 0, 50, 100, 250, 500, and 1000 nM. All data are presented as the mean  $\pm$  SEM (\* $P$  < 0.05, \*\* $P$  < 0.001, \*\*\* $P$  < 0.005 by unpaired two-tailed Student’s t-test)

**Inhibition of NCAM1 expression and formation of NCAM1–MHC-I complexes in AD**

Since NCAM1 is a novel interacting partner of neuronal MHC-I– $\beta_2$ M complex (Fig. 3) and MHC-I– $\beta_2$ M is destabilized by A $\beta$  oligomers and in AD brains (Figs. 1, 2), we speculated that the interaction of NCAM1 with MHC-I– $\beta_2$ M complex is also deregulated. As expected, co-immunoprecipitation assay showed reduction in the amount of NCAM1–MHC-I– $\beta_2$ M complex in AD brains (Fig. 4A, B). In primary neurons, NCAM1

co-localized with MHC-I at the surface of the soma or dendrites, however A $\beta$  oligomer reduced the co-localization intensity between MHC-I and NCAM1 or each protein levels (Fig. 4C–E). A $\beta$  treatment reduced the amount of NCAM1 interacting with MHC-I by about 50% relative to control in primary neurons (Fig. 4F, G). A $\beta$  treatment also reduced CREB phosphorylation, which is part of the final cascade of NCAM1 signaling (Fig. 4H, I), suggesting that the MHC-I– $\beta_2$ M complex

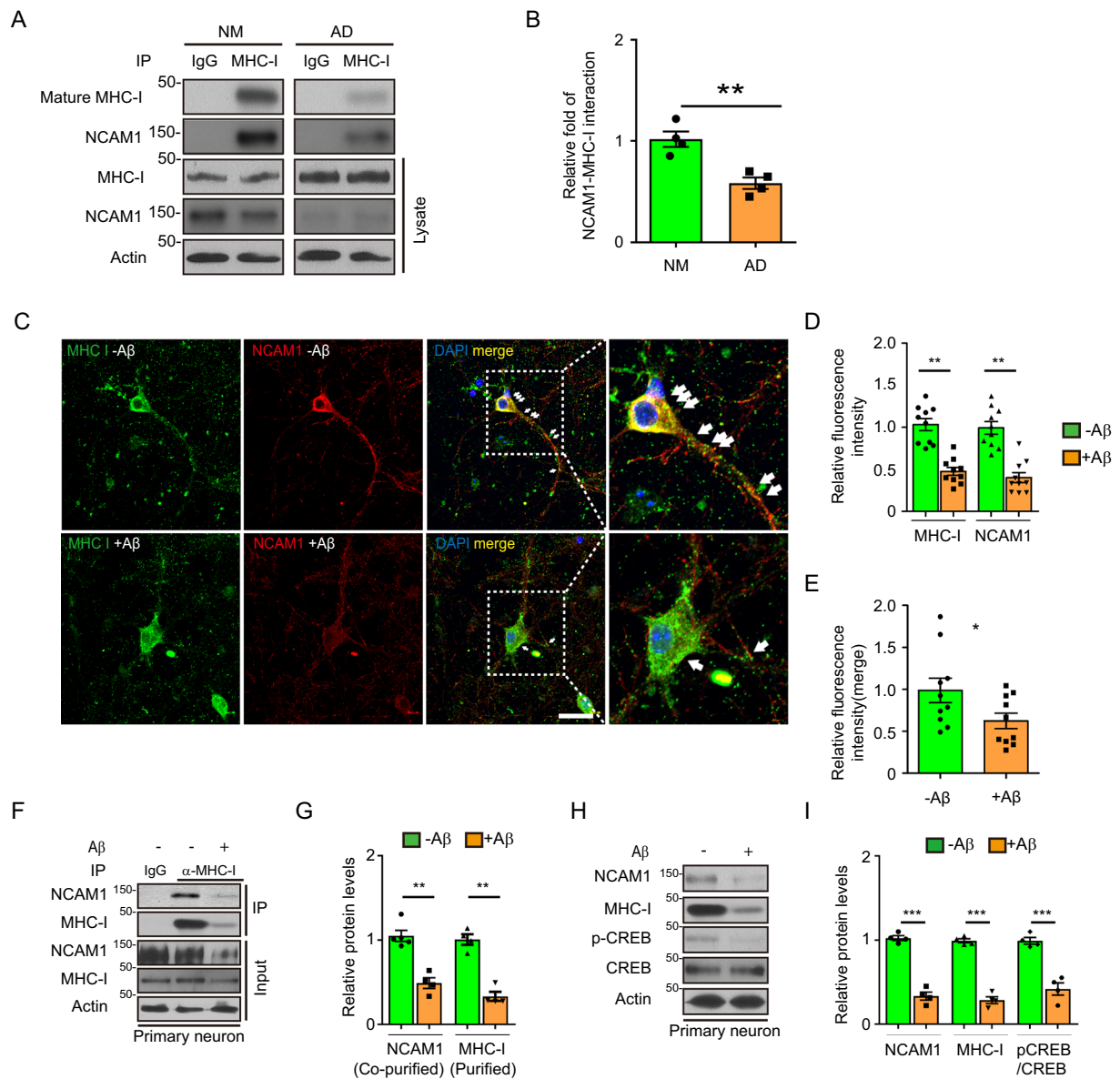


**Fig. 4** Impaired NCAM1–MHC-I interaction in AD pathology. **A, B** Co-immunoprecipitation analysis of interactions between endogenous MHC-I and NCAM1 in the brains of normal subjects (NM) and patients with AD (**A, B**; n = 4). The levels of co-immunoprecipitated NCAM1 were normalized to total NCAM1 levels (**B**). The data are presented as the mean ± SEM (\*\**P* < 0.001; unpaired two-tailed Student’s *t*-test). **C–E** Co-localization of MHC-I with NCAM1 on primary neurons. Scale bar: 10 μm (**C**). Relative fluorescence intensity of either MHC-I or NCAM1 (**D**) and colocalization of MHC-I and NCAM1 (**F, G**). Coimmunoprecipitation analysis of interactions between endogenous MHC-I and NCAM1 in oligomeric Aβ-treated primary neurons (**F**, n = 4). The levels of coimmunoprecipitated NCAM1 and MHC-I were normalized to the levels of total NCAM1 and MHC-I, respectively (**G**). (**H, I**) Oligomeric Aβ-mediated downregulation of NCAM1 signaling detected by CREB phosphorylation (**H**, n = 4). The levels of NCAM1, MHC-I, and phosphorylated CREB were normalized to the levels of total NCAM1, MHC-I, and CREB, respectively (**I**). All data are presented as the mean ± SEM (\**P* < 0.05, \*\**P* < 0.001, \*\*\**P* < 0.0005 by unpaired two-tailed Student’s *t*-test)

is important for interacting with NCAM1 and activating its signaling. Together, these observations suggested that Aβ-mediated destabilization of MHC-I-β2M complex eventually impairs the formation of NCAM1-MHC-I-β2M complex, subsequently dysregulating NCAM1 signaling.

**Stabilization of MHC-I-β2M complex rescued Aβ-mediated MHC-I depletion and dysregulation of NCAM1-MHC-I interactions**

To determine whether inhibition of Aβ-mediated dissociation of MHC-I-β2M complex can rescue downregulated

NCAM1 signaling through a recovery of interactions between MHC-I and NCAM1, we utilized a single-chain trimer (SCT) of MHC-I as an Aβ-resistant MHC-I-β2M complex. SCT, a synthetic gene encoding a sequential link of three cDNAs with peptide, β2M, and MHC-I heavy chains (HLA-A2.1 allele) (Fig. 5A) [38], was expressed on the cell surface of SH-SY5Y cells (Fig. 5B). Treatment of SH-SY5Y cells expressing the SCT form of MHC-I-β2M complex with Aβ had no effect on the surface and total levels of expression of SCT. This treatment, however, reduced the total and surface expression of endogenous MHC-I (Fig. 5B–D), demonstrated that

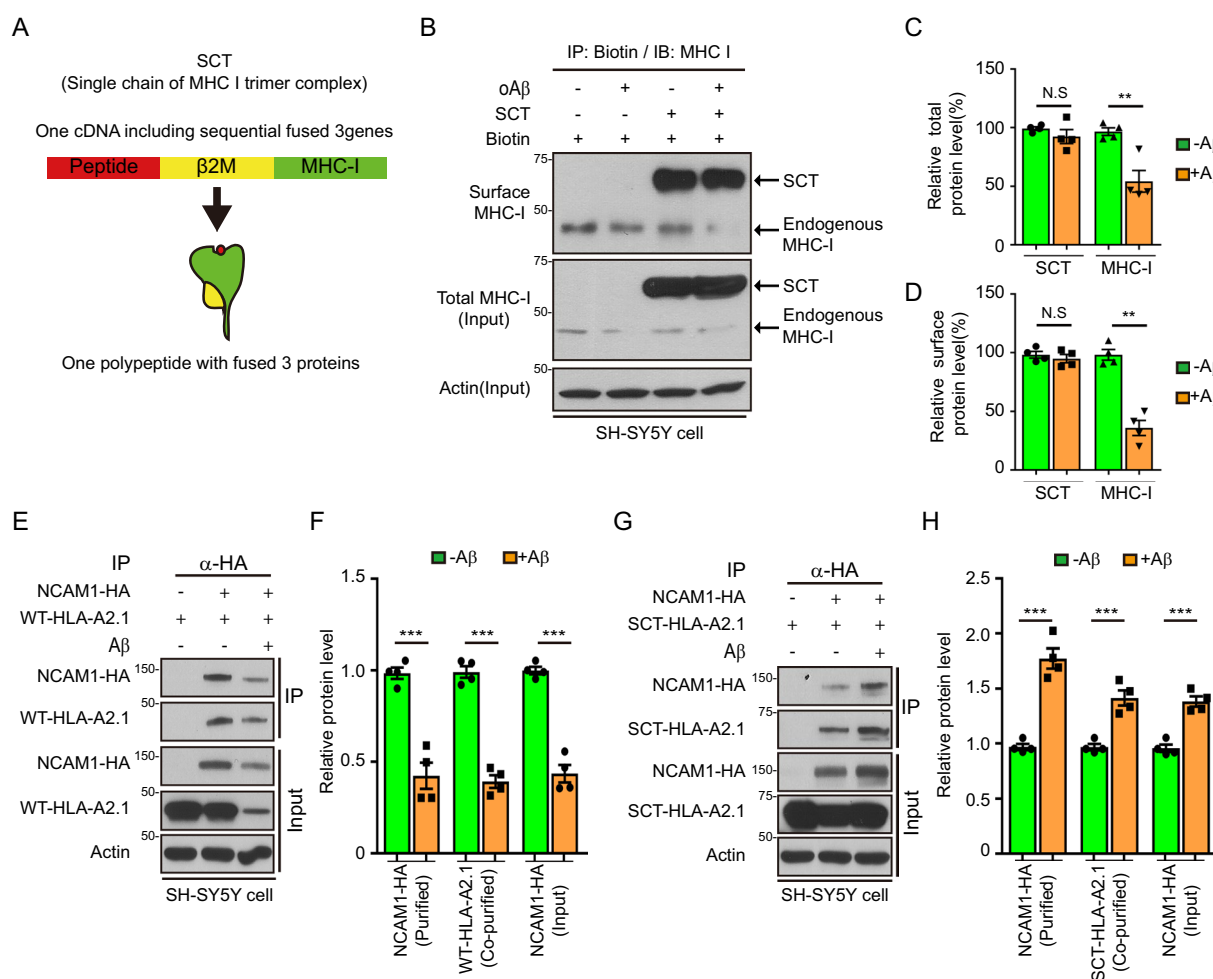


**Fig. 5** Aβ-resistance of MHC-I increased the interaction of NCAM1–MHC-I. **A** Schematic representation of the structure of the single-chain trimer (SCT). The SCT construct was composed of three genes (MHC-I, β<sub>2</sub>M, and antigen peptide), which resulted in the expression of a single protein composed of these three proteins. **B–D** Immunoblot analyses of endogenous MHC-I and exogenous SCT levels in oAβ-treated SH-SY5Y cells. Biotinylated surface MHC-I and SCT were immunoprecipitated with streptavidin and analyzed by immunoblotting (**B**, n=4). The levels of total (**C**) and surface (**D**) MHC-I and SCT were normalized to the levels of actin. The data were analyzed by unpaired two-tailed Student’s t-test (**C, D**). **E–H** Coimmunoprecipitation analysis of exogenous HLA-A2.1–NCAM1-HA (**E, F**; n=4) and SCT–NCAM1-HA (**G, H**; n=4) interactions in oAβ-treated SH-SY5Y cells. The levels of coimmunoprecipitated NCAM1-HA (**F, H**), HLA-A2.1 (**F**), and SCT (**H**) were normalized to actin levels, and the data were analyzed by unpaired two-tailed Student’s t-test (**F, H**). The data are presented as the mean ± SEM (N.S., not significant; \*P < 0.05, \*\*P < 0.001, \*\*\*P < 0.005)

the SCT form was resistant to destabilization by Aβ. In addition, Aβ-resistant SCT expression was able to protect MHC-I-NCAM1 interaction from the effects of Aβ treatment. Co-immunoprecipitation assays showed that levels of HLA-A2.1-SCT were resistant to Aβ treatment, resulting in a 1.5-fold increase in complexes of HLA-A2.1-SCT and NCAM1-HA (Fig. 5G, H). However, the HLA-A2.1-WT(wild-type) form was sensitive to Aβ and unable to interact with NCAM1-HA (Fig. 5E, F). Importantly, Aβ-mediated NCAM1 depletion was inhibited by expression of HLA-A2.1-SCT but not by HLA-A2.1-WT (Fig. 5E–H), suggesting that Aβ-mediated NCAM1 depletion depended on the Aβ-resistance of MHC-I-β<sub>2</sub>M complexes. To investigate whether the enhanced SCT-NCAM1 interaction can augment NCAM1 signaling for neurite outgrowth when treated with Aβ, primary neurons co-expressing green-fluorescent protein (GFP) and HLA-A2.1-WT or HLA-A2.1-SCT were treated with vehicle or Aβ (Fig. 6A), and NCAM1 signaling activity was assessed by measuring dendrite number and total length of neuronal processes of GFP-positive neurons

after eight divisions. Compared with vehicle treatment, Aβ treatment reduced dendrite numbers and lengths of neuronal processes in GFP expressing neurons (Fig. 6B, C). Notably, HLA-A2.1-SCT expression increased neurite density compared with HLA-A2.1-WT expression and GFP control when treated with Aβ, whereas HLA-A2.1-WT expression did not affect neuronal growth under the same conditions (Fig. 6A–C). These results suggested that the enhanced stability of the MHC-I-β<sub>2</sub>M complex ameliorated the Aβ-mediated downregulation of NCAM1 signaling in synaptic outgrowth.

### Discussion

The present study revealed that Aβ oligomers destabilizes synaptic MHC-I-β<sub>2</sub>M complex, impairing the interaction with NCAM-1, a novel MHC-I partner. We here further showed that inhibiting the Aβ-induced destabilization of MHC-I complex by SCT can reverse the neuronal signaling impairment, harnessing a novel therapeutic strategy.

Although studies have been made about the role of neuronal MHC-I in synaptic plasticity [6, 7, 39, 40], little

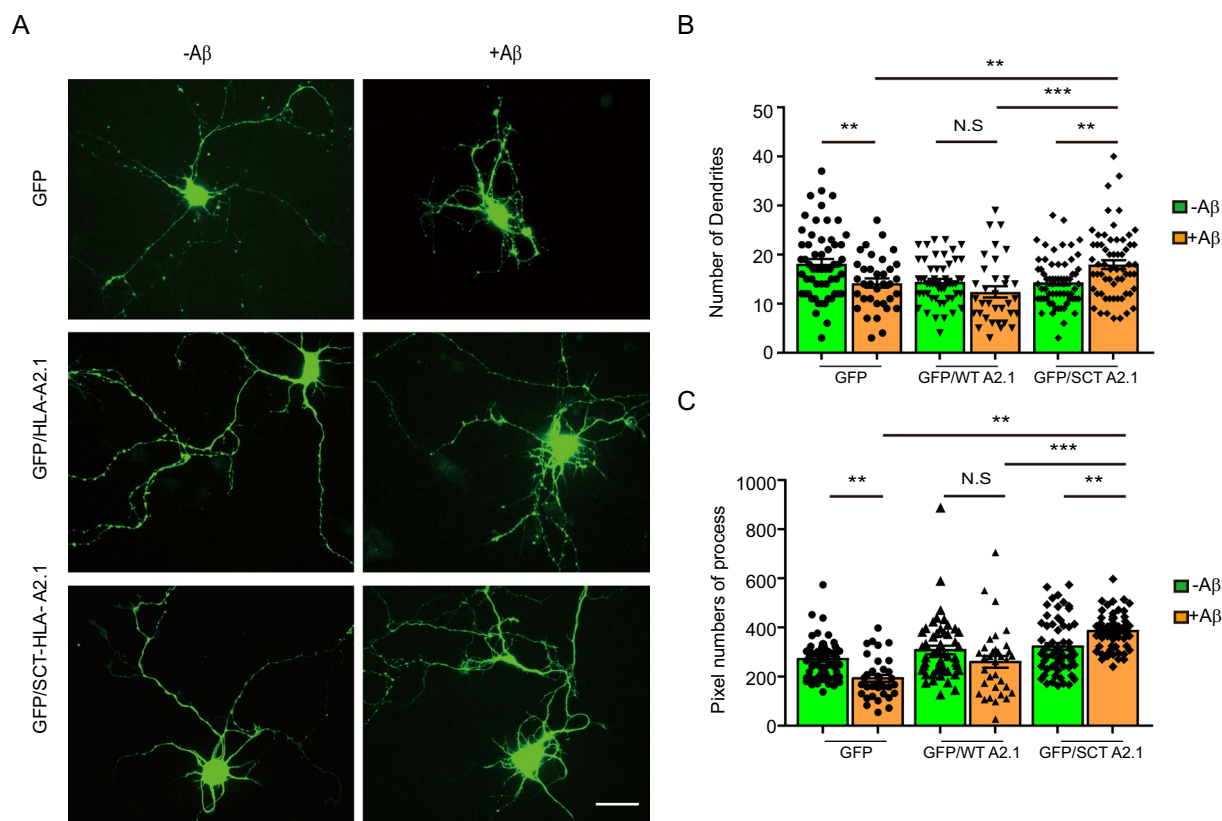


**Fig. 6** Aβ-resistance of MHC-I inhibited the Aβ-mediated downregulation of NCAM1 signaling. **A–C** Representative images of primary neurons expressing green-fluorescent protein (GFP), GFP/HLA-A2.1, and GFP/SCT-HLA-A2.1 in the presence or absence of treatment with oAβ for 8 days in vitro (**A**). Quantification of dendrite numbers (**B**) and the process lengths (**C**) in mock- and Aβ-treated primary neurons expressing GFP, GFP/HLA-A2.1, and GFP/SCT-HLA-A2.1 (n = 3, at least 35 segments per sample; two-way ANOVA with Tukey’s post-hoc comparisons test). Scale bar: 20 μm. The data are presented as the mean ± SEM (N.S., not significant; \*P < 0.05, \*\*P < 0.001, \*\*\*P < 0.005)

was known about MHC-I function in neurological diseases. Especially, the connection between MHC-I function and its role in AD remained unclear, despite genetic analyses showing an increased frequency of some MHC-I alleles in individuals with AD [10]. We here found that the unstable  $\beta$ 2M-free MHC-I heavy chain was increased in AD brains (Fig. 2). The oligomeric A $\beta$  was largely responsible for the destabilization of neuronal MHC-I- $\beta$ 2M complexes (Fig. 1). A $\beta$  treatment caused MHC-I- $\beta$ 2M complex to degenerate into soluble  $\beta$ 2M and  $\beta$ 2M-free MHC-I heavy chain, leading to rapid internalization of MHC-I heavy chain followed by lysosomal degradation (Fig. 1). This  $\beta$ 2M-free MHC-I heavy chain was also found to regulate synapse density negatively in glutamatergic neurons [7], which may be related with synapse loss in AD brains. MHC-I was also recently reported to be involved in the pathogenic mechanisms of the strongest risk factor of sporadic AD, apolipoprotein-E4 [41].

A $\beta$  oligomers induced extracellular release of  $\beta$ 2M which was dissociated from surface MHC-I- $\beta$ 2M complex (Fig. 1E, H). Several proteomics analyses have identified  $\beta$ 2M as a potential biomarker in the CSF of patients with AD [42, 43]. Interestingly,  $\beta$ 2M is a pro-aging factor that impairs cognitive function and neurogenesis, implying relations with AD [44].  $\beta$ 2M could induce cognitive decline via neuroinflammation through toll-like receptor 4 (TLR4) [45]. Hence, the increased release of  $\beta$ 2M downstream from A $\beta$ -induced dissociation of MHC-I- $\beta$ 2M complex (Fig. 1) could be related with neuroinflammation and neurodegeneration in AD. How A $\beta$  oligomer dissociates MHC-I- $\beta$ 2M complex is yet uncertain. A $\beta$  oligomer might dissociate MHC-I complex directly or indirectly via unknown mechanisms. Leukocyte immunoglobulin like receptor B2 (LilrB2) is a well-known binding partner with MHC-I [46]. A $\beta$  oligomers bind to LilrB2 [18], which might be a way of dissociating MHC-I- $\beta$ 2M complex indirectly. LilrB2 has a binding preference to  $\beta$ 2M-free MHC-I heavy chains rather than the MHC-I- $\beta$ 2M complex in vitro [47]. Additional studies are required to assess the detailed mechanism of MHC-I dissociation and toxic effects of A $\beta$ -mediated extracellular  $\beta$ 2M.

Because the function of MHC-I is mainly dependent on the protein with which it interacts, the identification of these proteins interacting with neuronal MHC-I is important for understanding MHC-I function in the CNS [3, 7]. We found here that NCAM1 protein is a novel functional receptor of MHC-I in the CNS (Fig. 3). NCAM1 is expressed in the adult CNS, is highly conserved in vertebrates, and is important for neurite outgrowth and synaptic plasticity in the

hippocampus [48, 49]. A $\beta$  decreased the interaction of NCAM1 with MHC-I, and NCAM1 downstream signaling (Fig. 4). Further investigation on the mechanism of NCAM decrease induced by A $\beta$  oligomers is required to elucidate role of MHC-I in NCAM stability. While independent effect of A $\beta$  oligomer on NCAM decrease is also possible, SCT-mediated MHC-I stabilization rescue of decreased NCAM levels and restoring synaptic levels suggest MHC-I-NCAM1 interaction role in protecting NCAM1 decrease by A $\beta$  oligomer (Fig. 5). NCAM, being a neuronal marker, is associated in AD. NCAM-deficient mice display reduced exploratory behavior and spatial learning, similar to the symptoms of AD in humans [50]. NCAM levels are lower in frontal and temporal cortex AD patients than control patients [51] and are increased in serum of AD patients [52]. A $\beta$  mediates the shedding of NCAM2, another neural cell adhesion molecule, leading to loss of glutamatergic synapses [53]. These results suggest that the overall stability of MHC-I is critical for its interaction with NCAM1 and potential role of MHC-I-NCAM1 interaction on pathogenesis of AD.

Various forms and alleles of MHC-I may regulate various synaptic functions via interactions with yet undetermined MHC-I receptors that can distinguish among MHC-I structures, suggesting the difference in regional or individual susceptibility of neurodegeneration in AD. The mechanisms regulating the transition of MHC-I structure and the identification of unidentified MHC-I interaction partners should be investigated further to understand the detailed functions of neuronal MHC-I.

## Conclusion

In summary, we report a novel pathological mechanism of AD, the A $\beta$ -mediated destabilization of the MHC-I- $\beta$ 2M complex and subsequent disruption of NCAM1 signaling. Furthermore, the SCT-mediated restoration of the MHC-I- $\beta$ 2M complex may be a promising therapeutic strategy for restoring synaptic function in AD patients.

## Abbreviations

MHC-I	Major histocompatibility complex I
AD	Alzheimer's disease
A $\beta$	$\beta$ -Amyloid
$\beta$ 2M	$\beta$ 2-Microglobulin
NCAM1	Neural cell adhesion molecule 1
CNS	Central nervous system
AMPA	$\alpha$ -Amino-3-hydroxy-5-methyl-4-isoxazolepropionic acid
NMDA	N-methyl-D-aspartate
FACS	Fluorescence-activated cell sorting
LC	Lactacystin

BFA1	Bafilomycin
M $\beta$ CD	Methyl- $\beta$ -cyclodextrin
CPZ	Chlorpromazine
ER	Endoplasmic reticulum
SCT	Single-chain trimer
LilrB2	Leukocyte immunoglobulin like receptor B2

## Supplementary Information

The online version contains supplementary material available at <https://doi.org/10.1186/s13578-023-01132-1>.

**Additional file 1: Figure S1.** Analysis of expression of the peptide-loading complex components and glycosylation maturation of MHC-I in AD. **A, B** Immunoblot analyses of the components of the peptide-loading complex (Erp57, PDI, tapasin, and TAP) in aged normal and AD brains (**A**;  $n = 3$  each). **B** The levels of Erp57, PDI, tapasin, and TAP were normalized to those of actin. **C** Intracellular MHC-I was immunoprecipitated from aged normal and AD brains, and digested with endoglycosidase-H (Endo-H) or peptide-N-glycosidase F (PNGase F). Glycosylated and deglycosylated forms of MHC-I were detected by immunoblotting. The data are presented as the mean  $\pm$  SEM (N.S., not significant; unpaired two-tailed Student's *t*-test).

**Additional file 2: Figure S2.** Identification of NCAM1 as an MHC-I interacting protein. **A** Summary of proteins identified as interacting with synaptic MHC-I- $\beta_2$ M complex. Proteins were aligned by id frequency. Previously identified MHC-I interacting proteins were based on the BioGRID database and labeled in red. **B** NCAM1 identified by liquid chromatography-tandem mass spectrometry (LC-MS/MS) analysis with 28 exclusive unique peptides and 38 exclusive unique spectra from 77 total spectra with 35% sequence coverage. The yellow-highlighted peptides are those detected by LC-MS/MS analysis. The green-highlighted "M" indicates an oxidated form of methionine. **C** The LC-MS/MS spectrum of "GLGEISAASEFK", a distinctive and representative peptide of NCAM1. The Y and B ions are displayed as blue and red peaks, respectively, and the green peaks indicate the immonium ions and internal cleaved ions.

**Additional file 3: Table S1.** Characteristics of the subjects assessed in this study. **Table S2.** Summary of top interactome of synaptic MHC-I- $\beta_2$ M complex.

## Acknowledgements

The authors thank Dr. Ted H. Hansen (Washington University School of Medicine, St. Louis, MO, USA) for generously providing the DNA construct expressing HLA-A2.1 SCT (TAX-HLA-A2.1-h $\beta$ M). The authors also thank the brain donors and their relatives for kindly providing the human brain materials, making these neuropathological studies possible. We also thank the core facilities of the Flowcytometry Core, Clinical Proteomics Core, and Laboratory of Animal Research at the Convergence mEDicine Research Center (CREDIT) of the Asan Medical Center for the use of their shared equipment, services, and expertise.

## Author contributions

MSK, KMC: data acquisition, statistical analyses, interpretation of results, and manuscript writing, MHC, NYK: data acquisition, statistical analyses, interpretation of results, KGK: data acquisition, statistical analyses, DHK, SYY: study conceptualization, interpretation of results, manuscript revising. The authors read and approved the final manuscript.

## Funding

This work was supported by the Basic Science Research Program through the National Research Foundation of Korea (NRF), which is funded by the Ministry of Science, ICT, & Future Planning (2018R1A5A2020732) and by a grant (2019IL0067) from the Asan Institute for Life Sciences, Seoul, Korea.

## Availability of data and materials

All data generated or analysed during this study are included in this published article.

## Declarations

### Ethics approval and consent to participate

All animal protocols were approved by the Institutional Animal Care and Use Committee at Asan Institute for Life Science in Seoul, Korea. Use of samples from Netherlands Brain Bank (NBB) were reviewed and approved by the NBB's scientific committee.

### Consent for publication

Not applicable.

### Competing interests

SYY founded ADEL and SYY, MSK, MHC, NYK, DHK own stocks or stock options of ADEL.

Received: 17 June 2023 Accepted: 11 September 2023

Published online: 29 September 2023

## References

- Peaper DR, Cresswell P. Regulation of MHC class I assembly and peptide binding. *Annu Rev Cell Dev Biol.* 2008;24:343–68.
- Cullheim S, Thams S. Classic major histocompatibility complex class I molecules: new actors at the neuromuscular junction. *Neuroscientist.* 2010;16(6):600–7.
- Shatz CJ. MHC class I: an unexpected role in neuronal plasticity. *Neuron.* 2009;64(1):40–5.
- Boulanger LM, Shatz CJ. Immune signalling in neural development, synaptic plasticity and disease. *Nat Rev Neurosci.* 2004;5(7):521–31.
- Corriveau RA, Huh GS, Shatz CJ. Regulation of class I MHC gene expression in the developing and mature CNS by neural activity. *Neuron.* 1998;21(3):505–20.
- Huh GS, Boulanger LM, Du H, Riquelme PA, Brotz TM, Shatz CJ. Functional requirement for class I MHC in CNS development and plasticity. *Science.* 2000;290(5499):2155–9.
- Glynn MW, Elmer BM, Garay PA, Liu XB, Needleman LA, El-Sabeawy F, McAllister AK. MHCI negatively regulates synapse density during the establishment of cortical connections. *Nat Neurosci.* 2011;14(4):442–51.
- Listi F, Candore G, Balistreri CR, Grimaldi MP, Orlando V, Vasto S, Colonna-Romano G, Lio D, Licastro F, Franceschi C, et al. Association between the HLA-A2 allele and Alzheimer disease. *Rejuvenation Res.* 2006;9(1):99–101.
- Lehmann DJ, Barnardo MC, Fuggle S, Quiroga I, Sutherland A, Warden DR, Barnettson L, Horton R, Beck S, Smith AD. Replication of the association of HLA-B7 with Alzheimer's disease: a role for homozygosity? *J Neuroinflammation.* 2006;3:33.
- Cifuentes RA, Murillo-Rojas J. Alzheimer's disease and HLA-A2: linking neurodegenerative to immune processes through an in silico approach. *Biomed Res Int.* 2014;2014:791238.
- Fourgeaud L, Davenport CM, Tyler CM, Cheng TT, Spencer MB, Boulanger LM. MHC class I modulates NMDA receptor function and AMPA receptor trafficking. *Proc Natl Acad Sci USA.* 2010;107(51):22278–83.
- Hsieh H, Boehm J, Sato C, Iwatsubo T, Tomita T, Sisodia S, Malinow R. AMPAR removal underlies Abeta-induced synaptic depression and dendritic spine loss. *Neuron.* 2006;52(5):831–43.
- Snyder EM, Nong Y, Almeida CG, Paul S, Moran T, Choi EY, Nairn AC, Salter MW, Lombroso PJ, Gouras GK, et al. Regulation of NMDA receptor trafficking by amyloid-beta. *Nat Neurosci.* 2005;8(8):1051–8.
- Syken J, Grandpre T, Kanold PO, Shatz CJ. PirB restricts ocular-dominance plasticity in visual cortex. *Science.* 2006;313(5794):1795–800.
- Adelson JD, Barreto GE, Xu L, Kim T, Brott BK, Ouyang YB, Naserke T, Djuricic M, Xiong X, Shatz CJ, et al. Neuroprotection from stroke in the absence of MHCI or PirB. *Neuron.* 2012;73(6):1100–7.
- Datwani A, McConnell MJ, Kanold PO, Micheva KD, Busse B, Shamloo M, Smith SJ, Shatz CJ. Classical MHCI molecules regulate retinogeniculate refinement and limit ocular dominance plasticity. *Neuron.* 2009;64(4):463–70.

17. Dickson HM, Zurawski J, Zhang H, Turner DL, Vojtek AB. POSH is an intracellular signal transducer for the axon outgrowth inhibitor Nogo66. *J Neurosci*. 2010;30(40):13319–25.
18. Kim T, Vidal GS, Djurisic M, William CM, Birnbaum ME, Garcia KC, Hyman BT, Shatz CJ. Human LILRB2 is a beta-amyloid receptor and its murine homolog PirB regulates synaptic plasticity in an Alzheimer's model. *Science*. 2013;341(6152):1399–404.
19. Braak H, Braak E. Neuropathological staging of Alzheimer-related changes. *Acta Neuropathol*. 1991;82(4):239–59.
20. Song HL, Shim S, Kim DH, Won SH, Joo S, Kim S, Jeon NL, Yoon SY. beta-Amyloid is transmitted via neuronal connections along axonal membranes. *Ann Neurol*. 2014;75(1):88–97.
21. Dunkley PR, Jarvie PE, Robinson PJ. A rapid Percoll gradient procedure for preparation of synaptosomes. *Nat Protoc*. 2008;3(11):1718–28.
22. Montealegre S, Venugopalan V, Fritzsche S, Kulicke C, Hein Z, Springer S. Dissociation of  $\beta$ 2-microglobulin determines the surface quality control of major histocompatibility complex class I molecules. *FASEB J*. 2015;29(7):2780–8.
23. Parham P, Barnstable CJ, Bodmer WF. Use of a monoclonal antibody (W6/32) in structural studies of HLA-A, B, C, antigens. *J Immunol*. 1979;123(1):342–9.
24. Stam NJ, Spits H, Ploegh HL. Monoclonal antibodies raised against denatured HLA-B locus heavy chains permit biochemical characterization of certain HLA-C locus products. *J Immunol*. 1986;137(7):2299–306.
25. Sugawara S, Abo T, Kumagai K. A simple method to eliminate the antigenicity of surface class I MHC molecules from the membrane of viable cells by acid treatment at pH 3. *J Immunol Methods*. 1987;100(1–2):83–90.
26. Ribic A, Zhang M, Schlumbohm C, Matz-Rensing K, Uchanska-Ziegler B, Flugge G, Zhang W, Walter L, Fuchs E. Neuronal MHC class I molecules are involved in excitatory synaptic transmission at the hippocampal mossy fiber synapses of marmoset monkeys. *Cell Mol Neurobiol*. 2010;30(6):827–39.
27. Goddard CA, Butts DA, Shatz CJ. Regulation of CNS synapses by neuronal MHC class I. *Proc Natl Acad Sci USA*. 2007;104(16):6828–33.
28. Shao CY, Mirra SS, Sait HB, Sacktor TC, Sigurdsson EM. Postsynaptic degeneration as revealed by PSD-95 reduction occurs after advanced Abeta and tau pathology in transgenic mouse models of Alzheimer's disease. *Acta Neuropathol*. 2011;122(3):285–92.
29. Sze CI, Troncoso JC, Kawas C, Mouton P, Price DL, Martin LJ. Loss of the presynaptic vesicle protein synaptophysin in hippocampus correlates with cognitive decline in Alzheimer disease. *J Neuropathol Exp Neurol*. 1997;56(8):933–44.
30. Elliott T, Williams A. The optimization of peptide cargo bound to MHC class I molecules by the peptide-loading complex. *Immunol Rev*. 2005;207:89–99.
31. Triantafyllou K, Fradelizi D, Wilson K, Triantafyllou M. GRP78, a coreceptor for coxsackievirus A9, interacts with major histocompatibility complex class I molecules which mediate virus internalization. *J Virol*. 2002;76(2):633–43.
32. Jackson MR, Cohen-Doyle MF, Peterson PA, Williams DB. Regulation of MHC class I transport by the molecular chaperone, calnexin (p88, IP90). *Science*. 1994;263(5145):384–7.
33. Park B, Lee S, Kim E, Chang S, Jin M, Ahn K. The truncated cytoplasmic tail of HLA-G serves a quality-control function in post-ER compartments. *Immunity*. 2001;15(2):213–24.
34. Kiss JZ, Muller D. Contribution of the neural cell adhesion molecule to neuronal and synaptic plasticity. *Rev Neurosci*. 2001;12(4):297–310.
35. Walmod PS, Kolkova K, Berezin V, Bock E. Zippers make signals: NCAM-mediated molecular interactions and signal transduction. *Neurochem Res*. 2004;29(11):2015–35.
36. Kleene R, Schachner M. Glycans and neural cell interactions. *Nat Rev Neurosci*. 2004;5(3):195–208.
37. Ronn LC, Berezin V, Bock E. The neural cell adhesion molecule in synaptic plasticity and ageing. *Int J Dev Neurosci*. 2000;18(2–3):193–9.
38. Yu YY, Netuschil N, Lybarger L, Connolly JM, Hansen TH. Cutting edge: single-chain trimers of MHC class I molecules form stable structures that potently stimulate antigen-specific T cells and B cells. *J Immunol*. 2002;168(7):3145–9.
39. Bilousova T, Dang H, Xu W, Gustafson S, Jin Y, Wickramasinghe L, Won T, Bobarnac G, Middleton B, Tian J, et al. Major histocompatibility complex class I molecules modulate embryonic neurogenesis and neuronal polarization. *J Neuroimmunol*. 2012;247(1–2):1–8.
40. McAllister AK. Major histocompatibility complex I in brain development and schizophrenia. *Biol Psychiatry*. 2014;75(4):262–8.
41. Zalocusky KA, Najm R, Taubes AL, Hao Y, Yoon SY, Koutsodendris N, Nelson MR, Rao A, Bennett DA, Bant J, et al. Neuronal ApoE upregulates MHC-I expression to drive selective neurodegeneration in Alzheimer's disease. *Nat Neurosci*. 2021;24(6):786–98.
42. Carrette O, Demalte I, Scherl A, Yalkinoglu O, Corthals G, Burkhard P, Hochstrasser DF, Sanchez JC. A panel of cerebrospinal fluid potential biomarkers for the diagnosis of Alzheimer's disease. *Proteomics*. 2003;3(8):1486–94.
43. Svatonova J, Borecka K, Adam P, Lanska V. Beta2-microglobulin as a diagnostic marker in cerebrospinal fluid: a follow-up study. *Dis Markers*. 2014;2014:495402.
44. Smith LK, He Y, Park JS, Bieri G, Snethlage CE, Lin K, Gontier G, Wabl R, Plambeck KE, Udeochu J, et al. beta2-microglobulin is a systemic pro-aging factor that impairs cognitive function and neurogenesis. *Nat Med*. 2015;21(8):932–7.
45. Zhong Q, Zou Y, Liu H, Chen T, Zheng F, Huang Y, Chen C, Zhang Z. Toll-like receptor 4 deficiency ameliorates  $\beta$ 2-microglobulin induced age-related cognition decline due to neuroinflammation in mice. *Mol Brain*. 2020;13(1):20.
46. Hudson LE, Allen RL. Leukocyte Ig-like receptors—a model for MHC class I disease associations. *Front Immunol*. 2016;7:281.
47. Shiroishi M, Kuroki K, Rasubala L, Tsumoto K, Kumagai I, Kurimoto E, Kato K, Kohda D, Maenaka K. Structural basis for recognition of the nonclassical MHC molecule HLA-G by the leukocyte Ig-like receptor B2 (LILRB2/LIR2/ILT4/CD85d). *Proc Natl Acad Sci USA*. 2006;103(44):16412–7.
48. Hall AK, Rutishauser U. Phylogeny of a neural cell adhesion molecule. *Dev Biol*. 1985;110(1):39–46.
49. Doherty P, Walsh FS. Cell adhesion molecules, second messengers and axonal growth. *Curr Opin Neurobiol*. 1992;2(5):595–601.
50. Brandewiede J, Stork O, Schachner M. NCAM deficiency in the mouse forebrain impairs innate and learned avoidance behaviours. *Genes Brain Behav*. 2014;13(5):468–77.
51. Aisa B, Gil-Bea FJ, Solas M, Garcia-Alloza M, Chen CP, Lai MK, Francis PT, Ramirez MJ. Altered NCAM expression associated with the cholinergic system in Alzheimer's disease. *J Alzheimers Dis*. 2010;20(2):659–68.
52. Todaro L, Puricelli L, Gioseffi H, Guadalupe Pallotta M, Lastiri J, de Kierjoffe EB, Varela M, Sacerdote de Lustig E. Neural cell adhesion molecule in human serum increased levels in dementia of the Alzheimer type. *Neurobiol Dis*. 2004;15(2):387–93.
53. Leshchynska I, Liew HT, Shepherd C, Halliday GM, Stevens CH, Ke YD, Ittner LM, Sytnyk V. Abeta-dependent reduction of NCAM2-mediated synaptic adhesion contributes to synapse loss in Alzheimer's disease. *Nat Commun*. 2015;6:8836.

## Publisher's Note

Springer Nature remains neutral with regard to jurisdictional claims in published maps and institutional affiliations.

**Ready to submit your research? Choose BMC and benefit from:**

- fast, convenient online submission
- thorough peer review by experienced researchers in your field
- rapid publication on acceptance
- support for research data, including large and complex data types
- gold Open Access which fosters wider collaboration and increased citations
- maximum visibility for your research: over 100M website views per year

**At BMC, research is always in progress.**

Learn more [biomedcentral.com/submissions](https://biomedcentral.com/submissions)

